

# Posterior Integration on an Embedded Riemannian Manifold

Chris. J. Oates<sup>\*†</sup>

April 6, 2022

## Abstract

This note extends the posterior integration method of Oates et al. (2016, 2017) to the case where the posterior is supported on an embedded Riemannian manifold. In contrast to the original Euclidean case, where certain boundary conditions are required, no boundary conditions are needed for a closed manifold. The important case of the 2-sphere is explored in detail.

**Keywords:** Bayesian computation, numerical integration, reproducing kernel, Stokes' theorem

## 1 Introduction

This work considers numerical approximation of an integral

$$\int_M f \, d\mathcal{P} \tag{1}$$

where  $M$  is a  $m$ -dimensional Riemannian manifold, for convenience assumed to be embedded in  $\mathbb{R}^d$ ,  $\mathcal{P}$  is a distribution suitably defined on  $M$  and  $f : M \rightarrow \mathbb{R}$  is a  $\mathcal{P}$ -measurable integrand. This fundamental problem is well-studied in applied mathematics and existing methods include Gaussian cubatures (Atkinson, 1982; Filbir and Mhaskar, 2010), cubatures based on uniformly-weighted quasi Monte Carlo points (Kuo and Sloan, 2005; Gräf, 2013) and cubatures based on optimally-weighted Monte Carlo points (Brandolini et al., 2010; Ehler and Gräf, 2017).

The numerical integration methods cited above assume that a closed form for  $\mathcal{P}$  is provided. However, this is not the case for many important integrals that occur in the applied

---

<sup>\*</sup>School of Mathematics, Statistics and Physics, Newcastle University, UK.

<sup>†</sup>Supported by the Lloyds Register Foundation programme on data-centric engineering at the Alan Turing Institute, UK.

statistical context. In particular, in the Bayesian framework the distribution  $\mathcal{P}$  can represent *posterior* belief: i.e.

$$\frac{d\mathcal{P}}{d\mathcal{P}_0}(\mathbf{x}) = \frac{\text{likelihood}(\mathbf{x})}{Z}$$

where  $\mathcal{P}_0$  is an expert-elicited *prior* distribution on  $M$  and a function, known as a *likelihood*, determines how the expert's belief should be updated on the basis of data obtained in an experiment; see Bernardo and Smith (2001) for the statistical background. The left hand side of this equation is to be interpreted as the Radon-Nikodym derivative of the posterior with respect to the prior (Stuart, 2010). Outside of conjugate exponential families, posterior distributions are not easily characterised, as the normalisation constant (or *marginal likelihood*)

$$Z = \int_M \text{likelihood}(\mathbf{x}) d\mathcal{P}_0(\mathbf{x})$$

is itself an intractable integral. Several methods for approximation of  $Z$  have been developed, but this problem is considered difficult – even in the case of the Euclidean manifold (see the survey in Friel and Wyse, 2012).

Integrals on manifolds arise in many important applications of Bayesian statistics, most notably directional statistics (Mardia and Jupp, 2000) and modelling of functional data on the sphere  $S^2$  (Porcu et al., 2016). The canonical scenario is that  $\mathcal{P}_0$  and  $\mathcal{P}$  admit densities  $\pi_0$  and  $\pi_{\mathcal{P}}$  with respect to the induced surface area (i.e. Hausdorff) measure  $\mathcal{H}$  on the manifold (i.e.  $d\mathcal{P}_0 = \pi_0 d\mathcal{H}$  and  $d\mathcal{P} = \pi_{\mathcal{P}} d\mathcal{H}$ ) and that a function proportional to this density can be provided (i.e. we are provided with a function  $\pi \propto \pi_{\mathcal{P}}$  but not  $\pi_{\mathcal{P}}$  itself). Specifically, in the context of Bayesian statistics on a Riemannian manifold, we are provided with

$$\pi(\mathbf{x}) = \text{likelihood}(\mathbf{x})\pi_0(\mathbf{x}).$$

How then should one attempt to approximate the integral in Eqn. 1? The obvious solution would be to form an approximation  $\hat{Z}$  to the normalising constant  $Z$  in order to recover an approximation  $\hat{\pi}_{\mathcal{P}} = \pi/\hat{Z}$  to  $\pi_{\mathcal{P}}$ , then to exploit an existing numerical integration method with  $\hat{\pi}_{\mathcal{P}}$  in place of  $\pi_{\mathcal{P}}$ . However, this is somewhat circular as  $Z$  itself is a challenging integral.

To provide a way forward, Markov chain Monte Carlo (MCMC) methods have been developed to sample from distributions defined on a manifold (Byrne and Girolami, 2013; Lan et al., 2014; Holbrook et al., 2016). These methods circumvent knowledge of  $Z$ , for instance by working only with the ratio  $\pi_{\mathcal{P}}(\mathbf{y})/\pi_{\mathcal{P}}(\mathbf{x}) = \pi(\mathbf{x})/\pi(\mathbf{y})$ . Their output is a realisation of an ergodic Markov process  $(\mathbf{x}_i)_{i=1}^n$  which leaves  $\mathcal{P}$  invariant, so that the integral may be approximated by the ergodic average  $\frac{1}{n} \sum_{i=1}^n f(\mathbf{x}_i)$  for sufficiently large  $n$  (Meyn and Tweedie, 2012). A drawback of MCMC – more pronounced in low dimensions – is the performance gap in terms of asymptotics between MCMC and methods that apply when  $\mathcal{P}$  can be fully characterised, with MCMC gated at  $O_P(n^{-1/2})$ . In essence, this is a consequence of the fact that MCMC methods do not exploit knowledge of smoothness properties of the integrand.

In recent years, several alternatives to MCMC have been developed to address this convergence bottleneck. These include transport maps (Marzouk et al., 2016), Riemann sums (Philippe and Robert, 2001), quasi Monte Carlo (Schwab and Stuart, 2012) and estimators based on Stein’s method (Oates et al., 2016; Liu and Wang, 2016; Oates et al., 2017). However, the methods which have so far been developed have focused on the case of the Euclidean manifold  $M = \mathbb{R}^d$ .

In this note we generalise one of these methods – the method studied in Oates et al. (2016, 2017) – for computation of posterior integrals on a general embedded Riemannian manifold. Inspired by classical cubature methods, the approach that we study proceeds in three steps: In the first step, the function  $\pi$  is exploited to construct a class  $H_\pi$  of functions, defined on the manifold, that can be exactly integrated with respect to  $\mathcal{P}$ . Next, the integrand  $f$  is approximated with a suitably chosen element  $\hat{f}$  from  $H_\pi$ . Finally, an estimate for the integral is given by the integral of the approximation to the integrand;  $\int_M \hat{f} d\mathcal{P}$ . The main technical contribution occurs in the first step, where we must elucidate the class  $H_\pi$  without access to  $Z$ , the normalisation constant. The main features of the proposed method are as follows:

- The approximation error is  $o(n^{-1/2})$  under regularity assumptions on the integrand. On the other hand, the computational cost of post-processing  $n$  evaluations of the integrand is up to  $O(n^3)$ .
- The points  $\{\mathbf{x}_i\}_{i=1}^n$  at which the integrand is evaluated do not need to form an approximation to  $\mathcal{P}$ . This can be useful if the points arise as a sample path from a Markov chain that has not converged.
- A computable upper bound on (relative) integration error - a *kernel Stein discrepancy* (Chwialkowski et al., 2016; Liu et al., 2016; Gorham and Mackey, 2017) - is provided. In fact, this is automatically computed as a by-product of approximating the integral.
- Compared to the original work in Oates et al. (2016, 2017) for the Euclidean manifold, non-trivial boundary conditions are not required on a closed manifold.

The remainder of the paper proceeds as follows: In Section 2 we provide a brief mathematical background. In Section 3 we present the proposed method. The method is empirically assessed in Section 4. Finally some further discussion of the approach is provided in Section 5.

## 2 Mathematical Background

The aim of this section is to present an informal and accessible introduction to some of the mathematical tools that are needed. For a formal treatment, several references to textbooks are provided.

**Embedded Riemannian Manifolds** Let  $M$  represent an  $m$ -dimensional manifold, embedded in  $\mathbb{R}^d$ . To avoid technical obfuscation, we will implicitly assume regularity conditions that ensure all mathematical objects exist and are well-defined. The manifold  $M$  can be characterised by a collection of coordinate systems: Let  $\mathbf{q} = (q_1, \dots, q_m) \in \mathbb{R}^m$  denote local coordinates and let  $\mathbf{x} = (x_1, \dots, x_d)$  denote coordinates for  $\mathbb{R}^d$ . Intuitively, for each  $\mathbf{x} \in M$  there exists a bijective map  $\nu : O_{\mathbb{R}^m} \rightarrow O_M$  from an open set  $\mathbf{q} \in O_{\mathbb{R}^m} \subset \mathbb{R}^m$  to an open set  $\mathbf{x} \in O_M \subset M$ . For such a map  $\nu$ , define the  $d \times m$  matrix

$$D_\nu = \begin{bmatrix} \frac{\partial \nu_1}{\partial q_1} & \cdots & \frac{\partial \nu_1}{\partial q_m} \\ \vdots & & \vdots \\ \frac{\partial \nu_d}{\partial q_1} & \cdots & \frac{\partial \nu_d}{\partial q_m} \end{bmatrix} = [\mathbf{v}_1, \dots, \mathbf{v}_m].$$

Note that  $D_\nu$  implicitly depends on position  $\mathbf{x} \in M$ . For  $\mathbf{x} \in M$ , define the tangent space  $T_{\mathbf{x}}M = \text{span}\{\mathbf{v}_1, \dots, \mathbf{v}_m\} \subset \mathbb{R}^d$ . An element of this space has the form  $a_1\mathbf{v}_1 + \dots + a_m\mathbf{v}_m$  and we denote such an element as  $\underline{\mathbf{a}} = (a_1, \dots, a_m)$ . Thus, as an abuse of notation, we can write  $\underline{\mathbf{a}} \in T_{\mathbf{x}}M$ . Note that  $D_\nu$  is a linear map from  $\mathbb{R}^m$  to  $T_{\mathbf{x}}M$ . Define the matrix  $G = D_\nu^\top D_\nu$  and the Jacobian  $J_\nu = \sqrt{\det(G)}$ . Note that  $J_\nu$  is the volume of the parallelepiped spanned by the columns  $\mathbf{v}_1, \dots, \mathbf{v}_m$  of  $D_\nu$ .

For each point  $\mathbf{x} \in M$ , the  $m \times m$  matrix  $G = G(\mathbf{x})$  defines an inner product on the tangent space  $T_{\mathbf{x}}M$ . Indeed, if  $\underline{\mathbf{a}}, \underline{\mathbf{b}} \in T_{\mathbf{x}}M$ , then  $\langle \underline{\mathbf{a}}, \underline{\mathbf{b}} \rangle_{G(\mathbf{x})} = \underline{\mathbf{a}}^\top G(\mathbf{x}) \underline{\mathbf{b}}$ . Thus, if we let

$$\begin{aligned} \mathbf{s} &= a_1\mathbf{v}_1 + \dots + a_m\mathbf{v}_m = D_\nu \underline{\mathbf{a}} \\ \mathbf{t} &= b_1\mathbf{v}_1 + \dots + b_m\mathbf{v}_m = D_\nu \underline{\mathbf{b}} \end{aligned}$$

then we see that  $\langle \underline{\mathbf{a}}, \underline{\mathbf{b}} \rangle_G = \underline{\mathbf{a}}^\top G \underline{\mathbf{b}} = \underline{\mathbf{a}}^\top D_\nu^\top D_\nu \underline{\mathbf{b}} = \langle \mathbf{s}, \mathbf{t} \rangle_2$ . Informally, the manifold  $M$  is said to be *Riemannian* if the inner product map  $\mathbf{x} \mapsto G(\mathbf{x})$  is smooth function of  $\mathbf{x} \in M$ .

**Calculus on a Riemannian Manifold** The Riemannian structure can be exploited to define gradients of functions and divergence of vector fields on the manifold. Indeed, let  $\underline{\mathbf{e}}_i = [0, \dots, 0, 1, 0, \dots, 0]^\top$  denote the coordinate basis vectors (n.b. these need not be orthonormal in the  $G$  inner product). Then we can define the gradient of a function  $f : M \rightarrow \mathbb{R}$  as

$$\nabla f = \sum_{i,j=1}^m [G^{-1}]_{i,j} \frac{\partial f}{\partial q_j} \underline{\mathbf{e}}_i$$

Likewise, define the divergence of a vector field  $\underline{\mathbf{s}} = s_1\underline{\mathbf{e}}_1 + \dots + s_m\underline{\mathbf{e}}_m$  to be

$$\nabla \cdot \underline{\mathbf{s}} = \sum_{i=1}^m \frac{\partial s_i}{\partial q_i} + s_i \frac{\partial}{\partial q_i} \log \sqrt{\det(G)}.$$

Both of the above expressions are coordinate invariant on the manifold.

**Geometric Measure Theory** In order to discuss densities on a general manifold, a reference measure – the Hausdorff measure, denoted  $\mathcal{H}$  – on the manifold must first be defined. The main concept here is that  $\mathcal{H}$  can be related to the standard Lebesgue measure  $\lambda^m$  on  $\mathbb{R}^m$ . Indeed, the measures  $\mathcal{H}$  and  $\lambda^m$  are connected via the *area formula*:

$$\int_A b(\nu(\mathbf{q})) J_\nu(\mathbf{q}) \lambda^m(d\mathbf{q}) = \int_{\mathbb{R}^n} b(\mathbf{x}) |\{\mathbf{q} \in A : \nu(\mathbf{q}) = \mathbf{x}\}| \mathcal{H}(d\mathbf{x})$$

whenever  $A$  is  $\lambda^m$  measurable and  $b : \mathbb{R}^d \rightarrow \mathbb{R}$  is Borel. Note that the left hand side is a standard Lebesgue integral, which is well-defined. If, in addition,  $\nu$  is a bijection then the right hand side is a surface integral over the set  $f(A)$ . Thus, intuitively,  $\mathcal{H}$  measures the surface area on  $M$ .

In the special case of a Riemannian manifold, the Hausdorff measure has the explicit form  $\mathcal{H}(d\mathbf{x}) = \sqrt{\det(G(\mathbf{x}))} \lambda^m(d\mathbf{q})$  (see Sec 3.2.46 of Federer, 1969). Thus the integral  $\int_U d\mathcal{H}$  can be defined for Borel subsets  $U \in \mathcal{B}(M)$ , and in this way  $\mathcal{H}$  induces a measure on  $(M, \mathcal{B}(M))$ . An excellent introduction to the role of Hausdorff measure in sampling can be found in Diaconis et al. (2013); Byrne and Girolami (2013).

**Stoke's Theorem on a Manifold** To rigorously formulate a manifold generalisation of the classical Stokes' theorem it is required to introduce concepts of differential forms, exterior products and exterior derivatives. To avoid technical obfuscation, we simply note that a 1-form is an object such as  $dq_i$  which can be integrated over a curve, a 2-form is an object such as  $dq_i dq_j$  which can be integrated over a surface, etc. Thus, for instance, the Hausdorff measure  $\mathcal{H}(d\mathbf{x}) = \sqrt{\det(G(\mathbf{x}))} \lambda^m(d\mathbf{q})$  is an  $m$ -form, as this can be integrated over the  $m$ -dimensional manifold. The *exterior derivative*  $dw$  of an  $(i-1)$ -form is an  $i$ -form; we refer the reader to e.g. Bachman (2006) for further background.

In the context of a general  $m$ -dimensional manifold, Stokes' theorem states that if  $w$  is an  $(m-1)$  form then

$$\int_M dw = \int_{\partial M} w$$

Thus if  $M$  is a closed manifold, then

$$\int_M dw = 0.$$

A somewhat technical point, which we state without comment, is that a gradient vector field  $\mathbf{s}$  corresponds to an  $(m-1)$ -form  $w = i_{\mathbf{s}} \mathcal{H}$  by *contracting*  $\mathbf{s}$  with the  $m$ -form  $\mathcal{H}$ . A classical text on this topic is Spivak (1971). The method proposed in Section 3 will use this fact to apply Stokes' theorem to the divergence of a particular gradient field.

**Reproducing Kernel Hilbert Spaces on a Manifold** The definition of a (real-valued) reproducing kernel Hilbert space (RKHS) on the manifold  $M$  is identical to the usual definition on the Euclidean manifold. Namely, an RKHS is a Hilbert space  $(H, \langle \cdot, \cdot \rangle_H)$  of functions  $H \ni h : M \rightarrow \mathbb{R}$  equipped with a *kernel*,  $k : M \times M \rightarrow \mathbb{R}$ , that satisfies:

1.  $k(\cdot, \mathbf{x}) \in H$  for all  $\mathbf{x} \in M$
2.  $k(\mathbf{x}, \mathbf{y}) = k(\mathbf{y}, \mathbf{x})$  for all  $\mathbf{x}, \mathbf{y} \in M$
3.  $\langle h, k(\cdot, \mathbf{x}) \rangle_H = h(\mathbf{x})$  for all  $h \in H, \mathbf{x} \in M$

For standard manifolds, such as the sphere  $S^2$ , several function spaces and their reproducing kernels have been studied (e.g. Porcu et al., 2016). For more general manifolds, the stochastic partial differential approach (Fasshauer and Ye, 2011; Lindgren et al., 2011) can be used to numerically approximate a suitable kernel.

Three important facts will be used later: First, the kernel  $k$  characterises the inner product  $\langle \cdot, \cdot \rangle_H$  and the set  $H$  consists of functions  $h$  with finite norm  $\|h\|_H = \langle h, h \rangle_H^{1/2}$ . Second, if  $H$  and  $\tilde{H}$  are two RKHS on  $M$  with reproducing kernels  $k$  and  $\tilde{k}$ , then  $H + \tilde{H}$  can be defined as the RKHS whose elements can be written as  $h + \tilde{h}$ ,  $h \in H, \tilde{h} \in \tilde{H}$ , with reproducing kernel  $k + \tilde{k}$ . Third, if  $L$  is a linear operator and  $H$  is an RKHS, then  $LH$  can be defined as the set  $LH = \{L(h) : h \in H\}$  endowed with the reproducing kernel  $L\bar{L}k(\mathbf{x}, \mathbf{y})$ , where  $\bar{L}$  denotes the adjoint of the operator  $L$ , which acts on the second argument  $\mathbf{y}$  rather than the first argument  $\mathbf{x}$ . See Berlinet and Thomas-Agnan (2011) for several examples of RKHS and additional technical background.

This completes our brief tour of the mathematical prerequisites; the next section describes the proposed posterior integration method.

### 3 Posterior Integration on a Riemannian Manifold

In this section we present the proposed numerical integration method. The approach that we study is similar to spline-based integration methods (e.g. the trapezoidal rule, Simpson's method, etc.) and proceeds in three main steps:

1. Using only  $\pi$  (i.e. not  $Z$ ), construct a flexible class  $H_\pi$  of functions  $h : M \rightarrow \mathbb{R}$  such that the integrals  $\int_M h \, d\mathcal{P}$  can be exactly computed.
2. Approximate the integrand  $f$  with a suitably chosen element  $\hat{f}$  from  $H_\pi$ .
3. Approximate the integral of interest as

$$\int_M f \, d\mathcal{P} \approx \int_M \hat{f} \, d\mathcal{P}.$$

It is clear that step 1 is the most non-trivial, since  $\mathcal{P}$  is not easily characterised with only knowledge of  $\pi$ , and this step will be our focus next.

**Step # 1: Constructing an Approximating Class  $H_\pi$**  The aim here is to construct a class  $H_\pi$  of functions whose integrals with respect to  $\mathcal{P}$  can be exactly computed. Crucially, this must proceed without knowledge of the (intractable) normalisation constant  $Z$ . To proceed, we generalise the method of Oates et al. (2016, 2017) to the case of a Riemannian manifold.

Let  $\Phi$  be a RKHS of suitably differentiable functions  $\phi : M \rightarrow \mathbb{R}$  whose reproducing kernel is denoted  $k$ . Then  $\underline{s} = \pi \nabla \phi$  denotes a gradient field on  $M$  and we may consider its divergence  $\nabla \cdot \underline{s}$  on  $M$ . In particular, consider the linear differential operator

$$L_\pi(\phi) := \frac{\nabla \cdot (\pi \nabla \phi)}{\pi}.$$

From Stokes' theorem we have that, if  $M$  is a closed manifold,

$$\begin{aligned} \int_M L_\pi(\phi) d\mathcal{P} &= \int_M \frac{\nabla \cdot (\pi \nabla \phi)}{\pi} \frac{\pi}{Z} d\mathcal{H} \\ &= \frac{1}{Z} \int_M \nabla \cdot (\pi \nabla \phi) d\mathcal{H} = 0 \end{aligned}$$

and thus  $L_\pi(\phi)$  can be exactly integrated. This follows since the integrand  $\nabla \cdot (\pi \nabla \phi) d\mathcal{H}$  is a differential  $m$ -form on  $M$ . Note that the same conclusion holds even when  $M$  is not closed, provided that  $\nabla \cdot (\pi \nabla \phi)$  vanishes everywhere on the boundary  $\partial M$ ; this is similar to the assumption made in Oates et al. (2016, 2017) for the case of the Euclidean manifold. Thus, for a closed manifold, the conditions needed for  $H_\pi$  to be exactly integrated are much simpler compared to earlier work.

The RKHS  $L_\pi \Phi$ , whose elements are functions of the form  $L_\pi(\phi)$ , is not flexible enough for our purposes, since these cannot approximate the function  $f(\mathbf{x}) = 1$ . Thus we augment  $L_\pi \Phi$  with the RKHS of constant functions, denoted  $\{1\}$  and with constant kernel  $\sigma^2$ , to obtain the function class

$$H_\pi = \{1\} + L_\pi \Phi.$$

Of course, the integral of the constant function with respect to a probability distribution is trivially computed. It follows that  $H_\pi$  is a RKHS with kernel

$$k_{\pi, \sigma}(\mathbf{x}, \mathbf{y}) = \sigma^2 + L_\pi \bar{L}_\pi k(\mathbf{x}, \mathbf{y}).$$

Under certain regularity assumptions, and additional technical details to deal with the fact that a slightly different differential operator was used, the set  $H_\pi$  can be shown to be dense in  $L_2(\mathcal{P})$  in the case of the Euclidean manifold (c.f. Lemma 4 of Oates et al., 2016). It is conjectured that this result holds also for a general Riemannian manifold.

**Step #2: Approximating the Integrand** Now that we have a class of functions  $H_\pi$  that can be exactly integrated, we must attempt to approximate  $f$  with an element from this set. Following Oates et al. (2016, 2017), the estimator that we consider is

$$\hat{f} = \arg \min_{h \in H_\pi} \|h\|_{H_\pi} \text{ s.t. } h(\mathbf{x}_i) = f(\mathbf{x}_i), i \in \{1, \dots, n\}.$$

From the representer theorem (see e.g. Schölkopf et al., 2001) it follows that  $\hat{f}$  has a closed form expression in terms of the kernel  $k_{\pi,\sigma}$ :

$$\hat{f}(\cdot) = [k_{\pi,\sigma}(\cdot, \mathbf{x}_1) \dots k_{\pi,\sigma}(\cdot, \mathbf{x}_n)] \underbrace{\begin{bmatrix} k_{\pi,\sigma}(\mathbf{x}_1, \mathbf{x}_1) & \dots & k_{\pi,\sigma}(\mathbf{x}_1, \mathbf{x}_n) \\ \vdots & & \vdots \\ k_{\pi,\sigma}(\mathbf{x}_n, \mathbf{x}_1) & \dots & k_{\pi,\sigma}(\mathbf{x}_n, \mathbf{x}_n) \end{bmatrix}}_{\mathbf{K}_{\pi,\sigma}}^{-1} \underbrace{\begin{bmatrix} f(\mathbf{x}_1) \\ \vdots \\ f(\mathbf{x}_n) \end{bmatrix}}_{\mathbf{f}}$$

This has the form of a weighted combination of functions in  $H_\pi$ :

$$\hat{f}(\cdot) = \sum_{i=1}^n w_i k_{\pi,\sigma}(\cdot, \mathbf{x}_i), \quad w_i = [\mathbf{K}_{\pi,\sigma}^{-1} \mathbf{f}]_i$$

The form of the estimator  $\hat{f}$  is rather standard can be characterised in several ways, e.g. as a Bayes rule for an  $L_2$  regression problem or as a posterior mean under a suitable Gaussian process regression model. Alternative kernel estimators, such as estimators that enforce non-negativity of the weights  $w_i$ , could be considered (c.f. Liu and Lee, 2017; Ehler and Gräf, 2017).

**Step #3: Approximating the Integral** The approximation  $\hat{f}$  can be exactly integrated:

$$\begin{aligned} \int_M \hat{f} \, d\mathcal{P} &= \sum_{i=1}^n w_i \int_M k_{\pi,\sigma}(\cdot, \mathbf{x}_i) \, d\mathcal{P} \\ &= \sigma^2 \sum_{i=1}^n w_i \\ &= \sigma^2 \mathbf{1}^\top \mathbf{K}_{\pi,\sigma}^{-1} \mathbf{f} \end{aligned} \tag{2}$$

The estimate in Eqn. 2 is recognised as a kernel quadrature method and, as such, it carries a Bayesian interpretation (Briol et al., 2016). Namely, from the Bayesian perspective, Eqn. 2 is the posterior mean for  $\int_M f \, d\mathcal{P}$  when  $f$  is modelled *a priori* as a centred Gaussian process with covariance function  $k_{\pi,\sigma}$  (see Rasmussen and Williams, 2006, for background on Gaussian process models). In this light, the parameter  $\sigma$  can be considered as a prior standard deviation for the value of the integral  $\int_M f \, d\mathcal{P}$ . Thus, since we may not know the size of the values taken by  $f$  in advance, we consider a weakly informative prior corresponding to the limit  $\sigma \rightarrow \infty$ . To this end, let  $k_\pi(\mathbf{x}, \mathbf{y}) = L_\pi \bar{L}_\pi k(\mathbf{x}, \mathbf{y})$  and let  $\mathbf{K}_\pi$  denote the kernel matrix with entries  $k_\pi(\mathbf{x}_i, \mathbf{x}_j)$ . Then the Woodbury matrix formula can be used to deduce



that

$$\begin{aligned}
\lim_{\sigma \rightarrow \infty} \int_M \hat{f} d\mathcal{P} &= \lim_{\sigma \rightarrow \infty} \sigma^2 \mathbf{1}^\top (\sigma^2 \mathbf{1} \mathbf{1}^\top + \mathbf{K}_\pi)^{-1} \mathbf{f} \\
&= \lim_{\sigma \rightarrow \infty} \sigma^2 \mathbf{1}^\top [\mathbf{K}_\pi^{-1} \mathbf{f} - \mathbf{K}_\pi^{-1} \mathbf{1} (\sigma^{-2} + \mathbf{1}^\top \mathbf{K}_\pi^{-1} \mathbf{1})^{-1} \mathbf{1}^\top \mathbf{K}_\pi^{-1} \mathbf{f}] \\
&= \lim_{\sigma \rightarrow \infty} \frac{\mathbf{1}^\top \mathbf{K}_\pi^{-1} \mathbf{f}}{\sigma^{-2} + \mathbf{1}^\top \mathbf{K}_\pi^{-1} \mathbf{1}} \\
&= \left( \frac{\mathbf{K}_\pi^{-1} \mathbf{1}}{\mathbf{1}^\top \mathbf{K}_\pi^{-1} \mathbf{1}} \right)^\top \mathbf{f}.
\end{aligned} \tag{3}$$

The estimator in Eqn. 3 is the one that is experimentally tested in Section 4. An interesting observation is that the weights  $w_i$  automatically sum to unity in this approach. Moreover, the expression  $(\mathbf{1}^\top \mathbf{K}_\pi^{-1} \mathbf{1})^{-1/2}$  is exactly the worst case error of the weighted point set  $\{(w_i, \mathbf{x}_i)\}_{i=1}^n$  in the unit ball of the RKHS  $H$  whose kernel is  $k_\pi$ :

$$(\mathbf{1}^\top \mathbf{K}_\pi^{-1} \mathbf{1})^{-1/2} = \sup \left\{ \left| \int_M f d\mathcal{P} - \lim_{\sigma \rightarrow \infty} \int_M \hat{f} d\mathcal{P} \right| : \|f\|_H \leq 1 \right\} \tag{4}$$

This quantity is also known as the *kernel Stein discrepancy* associated with the weighted point set  $\{(w_i, \mathbf{x}_i)\}_{i=1}^n$  (Chwialkowski et al., 2016; Liu et al., 2016; Gorham and Mackey, 2017). Thus a measure of (relative) integration error comes for free when the estimator is computed. From standard duality, this expression is also the posterior standard deviation for the integral. Of course, in practice the linear system  $\mathbf{K}_\pi^{-1} \mathbf{1}$  need only be solved once, at a cost of at most  $O(n^3)$ .

**Comparison to Earlier Work** The earlier work of Oates et al. (2016, 2017) considered an arbitrary vector field  $\phi$  in place of the gradient field  $\nabla \phi$ , and thus required only a first order differential operator. This was possible since the coordinates of the vector field can be dealt with independently in the case of the Euclidean manifold, but this will not be possible in the case of a general manifold. Interestingly, the second order differential operator considered here is the manifold generalisation of the operator used in the earlier work of Assaraf and Caffarel (1999); Mira et al. (2013). Other so-called *Stein* operators are discussed in Gorham et al. (2016).

## 4 Numerical Assessment

In this section we report the results from a simulation study designed to assess the performance of the proposed numerical method. In Section 4.1 we first return to the standard case of the Euclidean manifold  $M = \mathbb{R}^d$ , then in Section 4.2 we present experiments performed on the sphere  $M = S^2$ .

## 4.1 Euclidean Manifold

First, we consider the Euclidean manifold  $M = \mathbb{R}^d$ . This is for two reasons; first, to expose the proposed construction in a familiar context, and second, to determine whether the use of a second order differential operator leads to any substantive differences relative to earlier work.

**Differential Operator** For  $M = \mathbb{R}^d$ , we have  $\mathbf{q} = \mathbf{x}$  and the Hausdorff measure is the Lebesgue measure;  $\mathcal{H}(\mathrm{d}\mathbf{x}) = \lambda^d(\mathrm{d}\mathbf{x})$ . For simplicity, suppose that either  $\pi$  vanishes on  $\partial M$  or  $M = \mathbb{R}^d$ . Then our method involves the second order differential operator

$$\begin{aligned} L_\pi(\phi) &= \frac{\nabla \cdot (\pi \nabla \phi)}{\pi} \\ &= \frac{\nabla \pi}{\pi} \cdot \nabla \phi + \Delta \phi \end{aligned}$$

where  $\nabla = [\partial_{x_1}, \dots, \partial_{x_d}]^\top$  is the familiar gradient. For the case where  $M$  is bounded, let  $\mathbf{n}(\mathbf{x})$  denote the unit normal to  $\partial M$  in the ambient space  $\mathbb{R}^d$ . Then from the Euclidean version of Stokes' theorem:

$$\begin{aligned} \int_M L_\pi(\phi) \, \mathrm{d}\mathcal{P} &= \int_{\partial M} \pi(\mathbf{x}) \nabla \phi(\mathbf{x}) \cdot \mathbf{n}(\mathbf{x}) \, \mathrm{d}\lambda^d(\mathbf{x}) \\ &= \int_{\partial M} 0 \, \mathrm{d}\lambda^d(\mathbf{x}) = 0. \end{aligned}$$

The final equality is trivial for the case  $M = \mathbb{R}^d$ . This is to be contrasted with the earlier work of Oates et al. (2016, 2017), which considered a general vector field  $\boldsymbol{\phi} : M \rightarrow \mathbb{R}^d$  and the first order differential operator

$$L_\pi^1(\boldsymbol{\phi}) = \frac{\nabla \cdot (\pi \boldsymbol{\phi})}{\pi}.$$

From there, Oates et al. (2016, 2017) proceed as we have already described, with  $\boldsymbol{\phi} \in \Phi \times \dots \times \Phi$  the tensor product of  $d$  copies of the RKHS  $\Phi$ . Note that  $L_\pi^1$  implicitly relies on the Euclidean structure of the manifold and is not general.

**Choice of Kernel** If  $\alpha \in \mathbb{N} + \frac{1}{2}$  then the Matérn kernel

$$k(\mathbf{x}, \mathbf{y}) = \lambda^2 \exp\left(-\frac{\sqrt{2\alpha}\|\mathbf{x} - \mathbf{y}\|}{\ell}\right) \frac{\Gamma(\alpha + \frac{1}{2})}{\Gamma(2\alpha)} \sum_{i=0}^{\alpha - \frac{1}{2}} \frac{(\alpha - \frac{1}{2} + i)!}{i!(\alpha - \frac{1}{2} - i)!} \left(\frac{\sqrt{8\alpha}\|\mathbf{x} - \mathbf{y}\|}{\ell}\right)^{\alpha - \frac{1}{2} - i}$$

with parameters  $\lambda, \ell > 0$  reproduces the Sobolev space  $\Phi = H^\alpha(\mathbb{R}^d)$  (see e.g. Fasshauer, 2007). In order for  $L_\pi \Phi$  to be well-defined, we require that elements of  $\Phi$  are twice (weakly) differentiable; hence we require that  $\alpha > 2$ . In contrast, for  $L_\pi^1$  to be well defined we have the weaker requirement that  $\alpha > 1$ .

```

1 % logarithm of the un-normalised measure pi
2 log_pi = @(x1,x2) - x1^2 - x2^2;
3
4 % Differential operator L_pi on the Euclidean manifold R^2
5 dq1 = @(f,x1,x2) diff(f,x1); % d/dq_1
6 dq2 = @(f,x1,x2) diff(f,x2); % d/dq_2
7 d2q1 = @(f,x1,x2) diff(f,x1,2); % d^2/dq_1^1
8 d2q2 = @(f,x1,x2) diff(f,x2,2); % d^2/dq_2^2
9 L = @(f,x1,x2) dq1(log_pi(x1,x2),x1,x2)*dq1(f,x1,x2) ...
10      + dq2(log_pi(x1,x2),x1,x2)*dq2(f,x1,x2) ...
11      + d2q1(f,x1,x2) ...
12      + d2q2(f,x1,x2);
13
14 % Radial basis function (alpha = 5/2)
15 matern = @(r) (1 + sqrt(5)*r + 5*r^2/3) * exp(-sqrt(5)*r);
16
17 % Reproducing kernel
18 syms x1 x2 y1 y2
19 k = matern(sqrt((x1-y1)^2 + (x2-y2)^2));
20
21 % Symbolic differentiation
22 L_k = L(k,x1,x2); % differentiate wrt [x1,x2]
23 L_Lbar_k = L(L_k,y1,y2); % differentiate wrt [y1,y2]

```

Figure 1: Symbolic differentiation was used to automate computation of the kernel  $k_\pi$ . [This code snippet is for the problem considered in Section 4.1 for  $d = 2$  dimensions. The differential operator was  $L_\pi$ .]

**Experimental Results** For a transparent and reproducible test bed, let  $\mathcal{P}$  be the standard Gaussian in  $\mathbb{R}^d$  and suppose that we are told  $\pi(\mathbf{x}) = \exp(-\|\mathbf{x}\|^2/2)$ . That is, we pretend that the normalisation constant  $(2\pi)^{d/2}$  is unknown and proceed as described. For the kernel we fixed  $\lambda = 1$ ,  $\ell = 1$  and considered values  $\alpha \in \{3/2, 5/2, 7/2\}$ . For the points  $\{\mathbf{x}_i\}_{i=1}^n$  we consider three scenarios:

1. independent, unbiased draws  $\mathbf{x}_i \sim \mathcal{N}(\mathbf{0}, \mathbf{I})$
2. independent, biased draws  $\mathbf{x}_i \sim \mathcal{N}(\mathbf{1}, 3\mathbf{I})$
3. (for  $d = 1$ ) stratified points  $\mathbf{x}_i$  = the  $\frac{i}{n+1}$ th percentile of  $\mathcal{N}(0, 1)$

For each point set we computed the worst case error in Eqn. 4. (For scenarios 1 and 2 we report the mean worst case error obtained over 100 independent realisations of the random points.) Both differential operators  $L_\pi$  and  $L_\pi^1$  were considered, although the former is incompatible with  $\alpha = 1/2$ .

All results were obtained using MATLAB R2017b, with symbolic differentiation exploited to compute all kernels  $k_\pi$ . An example code snippet is provided in Fig. 1; it should be noted

that only lines 5-12 depend on the geometry of the manifold, and these are independent of both  $\pi$  and  $k$ . Thus, generic code for (e.g.) the sphere  $S^2$  can be provided.

Results, in Fig. 2 for  $d = 1$  and 3 for  $d = 2$ , showed that:

- Larger smoothness  $\alpha$  leads to faster decay of worst case error. In particular, we see a clear improvement compared to the  $O_P(n^{-1/2})$  of MCMC. In the case of the operator  $L_\pi^1$  studied on the Euclidean manifold in Oates et al. (2016) (right column), it was proven (under some additional assumptions) that the worst case error decreases at  $O(n^{-(\alpha-1)/d})$  when  $\pi$  is smooth, essentially because the kernel  $k_{\pi,\sigma}$  has smoothness  $\alpha - 1$ . This is consistent with the experimental results in Fig. 2. A small extension of the theoretical methods used in Oates et al. (2016) gives a corresponding rate for the operator  $L_\pi$  of  $O(n^{-(\alpha-2)/d})$ , since  $L_\pi$  is a second order differential operator. The results in the left column of Fig. 2 bear out this conjecture, with slower convergence of the worst case error for fixed  $\alpha$  compared to the right column.
- There was only a small difference between the worst case error in the first scenario ( $\mathbf{x}_i \sim \mathcal{N}(0, 1)$ , top row) compared to the second scenario ( $\mathbf{x}_i \sim \mathcal{N}(1, 3)$ , middle row). This clearly illustrates the property that the points  $\{\mathbf{x}_i\}_{i=1}^n$  need not form an approximation to  $\mathcal{P}$  in the proposed method. On the other hand, the stratified points (bottom row) appeared to mitigate the transient phase before the linear asymptotics kicks in, compared to the use of Monte Carlo points, and should be preferred.
- In dimension  $d = 2$  the worst case error decays more slowly, consistent with the rates just conjectured. Moreover, the asymptotic advantage of larger  $\alpha$  is not clearly seen for  $n \leq 10^2$  so that the transient phase appears to last for longer. This is consistent with the well-known curse of dimension for isotropic kernel methods.

## 4.2 The Sphere $S^2$

Next we considered arguably the most important non-Euclidean manifold; the sphere  $S^2$ . Recall that the sphere is (almost everywhere) parametrised in spherical coordinates  $\mathbf{q} = (q_1, q_2)$  as

$$(x_1, x_2, x_3) = \nu(\mathbf{q}) = (\cos q_1 \sin q_2, \sin q_1 \sin q_2, \cos q_2)$$

where  $q_1 \in [0, 2\pi)$  and  $q_2 \in [0, \pi]$ . It is thus a  $m = 2$  dimensional manifold embedded in  $\mathbb{R}^3$ .

**Differential Operator** The coordinate map  $\nu$  can be used to compute the metric tensor

$$\mathbf{G} = \begin{pmatrix} \sin^2 q_2 & 0 \\ 0 & 1 \end{pmatrix},$$

which can be recovered as  $\mathbf{G} = \mathbf{D}_\nu^\top \mathbf{D}_\nu$ . This leads to the Jacobian  $J_\nu = \sin q_2$  and thus a volume element  $\sin q_2 \, dq_1 dq_2$ . It follows that, for a function  $\phi : S^2 \rightarrow \mathbb{R}$ , we have the gradient

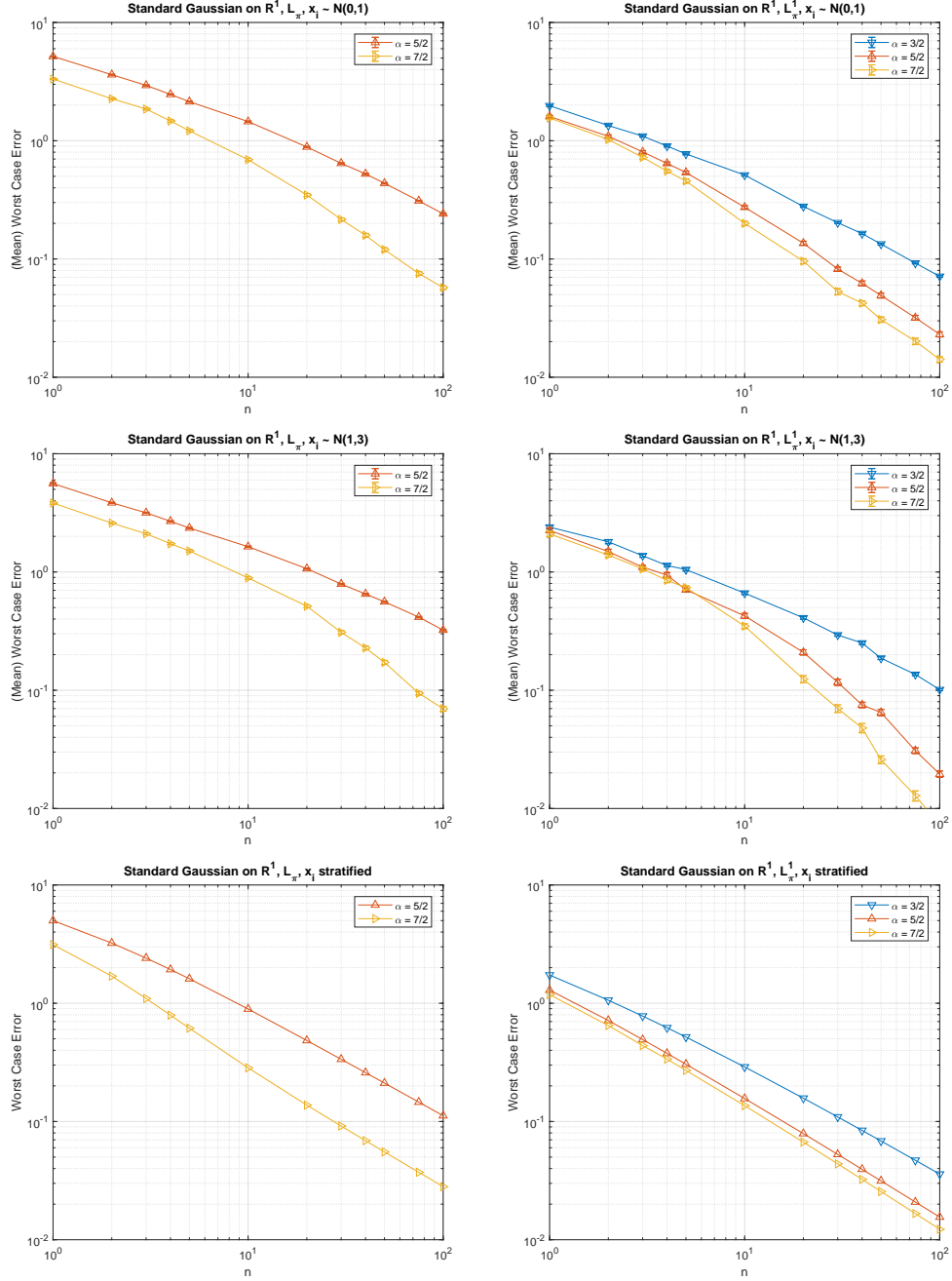


Figure 2: Results for the standard Gaussian on the Euclidean manifold in dimension  $d = 1$ . The worst case error of the proposed method is plotted for various  $\alpha$ , controlling the smoothness of the kernel, and various  $n$ , the number of evaluations of the integrand. [Top row: The points  $\mathbf{x}_i \sim \mathcal{N}(0,1)$  are drawn from the target. Middle row: The points  $\mathbf{x}_i \sim \mathcal{N}(1,3)$  are drawn from an incorrect distribution. Bottom row: The points  $\mathbf{x}_i$  were stratified on the percentiles of the target. Left column: The differential operator  $L_\pi$  considered in this work. Right column: The differential operator  $L_\pi^1$  considered in earlier work.]

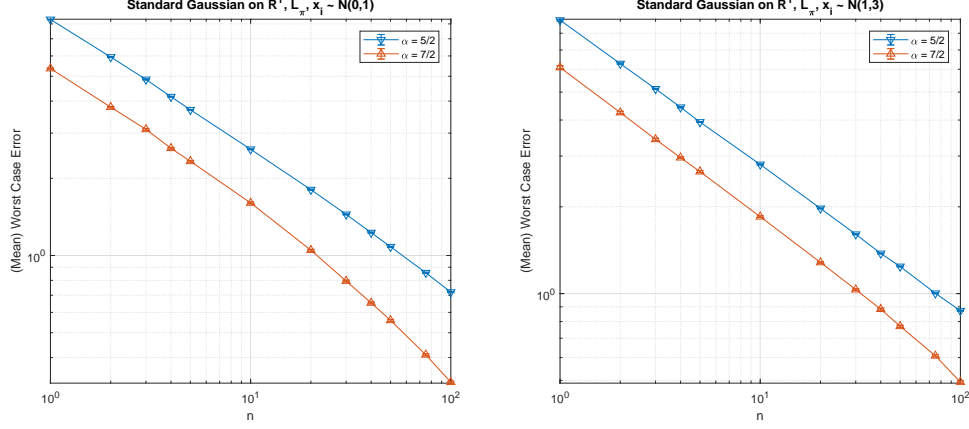


Figure 3: Results for the standard Gaussian on the Euclidean manifold in dimension  $d = 2$ . The worst case error of the proposed method is plotted for various  $\alpha$ , controlling the smoothness of the kernel, and various  $n$ , the number of evaluations of the integrand. [Left: The points  $\mathbf{x}_i \sim \mathcal{N}(0, 1)$  are drawn from the target. Right: The points  $\mathbf{x}_i \sim \mathcal{N}(1, 3)$  are drawn from an incorrect distribution. In each case the differential operator  $L_\pi$  was used.]

differential operator

$$\begin{aligned} \nabla f &= \sum_{i,j=1}^m [G^{-1}]_{i,j} \frac{\partial \phi}{\partial q_j} \mathbf{e}_i \\ &= \frac{1}{\sin^2 q_2} \frac{\partial \phi}{\partial q_1} \mathbf{e}_1 + \frac{\partial \phi}{\partial q_2} \mathbf{e}_2. \end{aligned}$$

Similarly, for a vector field  $\underline{\mathbf{s}} = s_1 \mathbf{e}_1 + \dots + s_m \mathbf{e}_m$ , we have the divergence operator

$$\begin{aligned} \nabla \cdot \underline{\mathbf{s}} &= \sum_{i=1}^m \frac{\partial s_i}{\partial q_i} + s_i \frac{\partial}{\partial q_i} \log \sqrt{\det(G)} \\ &= \frac{\partial s_1}{\partial q_1} + \frac{\partial s_2}{\partial q_2} + \frac{\cos q_2}{\sin q_2} s_2. \end{aligned}$$

Thus the linear operator  $L_\pi$  that we consider is:

$$\begin{aligned} L_\pi(\phi) &:= \frac{\nabla \cdot (\pi \nabla \phi)}{\pi} = \frac{1}{\pi} \frac{1}{\sin^2 q_2} \frac{\partial}{\partial q_1} \left\{ \pi \frac{\partial \phi}{\partial q_1} \right\} + \frac{1}{\pi} \frac{\partial}{\partial q_2} \left\{ \pi \frac{\partial \phi}{\partial q_2} \right\} + \frac{\cos q_2}{\sin q_2} \frac{\partial \phi}{\partial q_2} \\ &= \frac{\cos q_2}{\sin q_2} \frac{\partial \phi}{\partial q_2} + \frac{1}{\sin^2 q_2} \left\{ \frac{1}{\pi} \frac{\partial \pi}{\partial q_1} \frac{\partial \phi}{\partial q_1} + \frac{\partial^2 \phi}{\partial q_1^2} \right\} + \left\{ \frac{1}{\pi} \frac{\partial \pi}{\partial q_2} \frac{\partial \phi}{\partial q_2} + \frac{\partial^2 \phi}{\partial q_2^2} \right\}. \end{aligned}$$

Turning this into expressions in terms of  $\mathbf{x}$  requires that we notice

$$\frac{\cos q_2}{\sin q_2} = \frac{x_3}{\sqrt{1 - x_3^2}}, \quad \frac{1}{\sin^2 q_2} = \frac{1}{1 - x_3^2}$$

```

1 % Differential operator L_pi on the sphere S^2
2 dq1 = @(f,x1,x2,x3) -x2*diff(f,x1) + x1*diff(f,x2); % d/dq_1
3 dq2 = @(f,x1,x2,x3) x1*x3*(1-x3^2)^(-1/2)*diff(f,x1) ...
4         + x2*x3*(1-x3^2)^(-1/2)*diff(f,x2) ...
5         - (1-x3^2)^(1/2)*diff(f,x3); % d/dq_2
6 d2q1 = @(f,x1,x2,x3) x2^2*diff(f,x1,2) ...
7         - 2*x1*x2*diff(f,x1,x2) ...
8         + x1^2*diff(f,x2,2) ...
9         - x1*diff(f,x1) ...
10        - x2*diff(f,x2); % d^2/dq_1^2
11 d2q2 = @(f,x1,x2,x3) x1^2*x3^2*(1-x3^2)^(-1)*diff(f,x1,2) ...
12        + 2*x1*x2*x3^2*(1-x3^2)^(-1)*diff(f,x1,x2) ...
13        - 2*x1*x3*diff(f,x1,x3) ...
14        + x2^2*x3^2*(1-x3^2)^(-1)*diff(f,x2,2) ...
15        - 2*x2*x3*diff(f,x2,x3) ...
16        + (1-x3^2)*diff(f,x3,2) ...
17        - x1*diff(f,x1) ...
18        - x2*diff(f,x2) ...
19        - x3*diff(f,x3); % d^2/dq_2^2
20 L = @(f,x1,x2,x3) x3*(1-x3^2)^(-1/2)*dq2(f,x1,x2,x3) ...
21        + (1-x3^2)^(-1)*dq1(log_pi(x1,x2,x3),x1,x2,x3)*dq1(f,x1,x2,x3) ...
22        + (1-x3^2)^(-1)*d2q1(f,x1,x2,x3) ...
23        + dq2(log_pi(x1,x2,x3),x1,x2,x3)*dq2(f,x1,x2,x3) ...
24        + d2q2(f,x1,x2,x3);

```

Figure 4: Symbolic differentiation was used to automate computation of the kernel  $k_\pi$ . [This code snippet is for the problem considered in Section 4.2, the sphere  $S^2$ . The differential operator was  $L_\pi$ .]

and use chain rule for partial differentiation:

$$\frac{\partial}{\partial q_i} = \sum_{j=1}^3 \frac{\partial x_j}{\partial q_i} \frac{\partial}{\partial x_j}$$

$$\frac{\partial^2}{\partial q_i^2} = \sum_{j,k=1}^3 \frac{\partial x_j}{\partial q_i} \frac{\partial x_k}{\partial q_i} \frac{\partial^2}{\partial x_j \partial x_k} + \sum_{j=1}^3 \frac{\partial^2 x_j}{\partial q_i^2} \frac{\partial}{\partial x_j}.$$

This manifold-specific portion of MATLAB code is presented in Fig. 4. Again, we emphasise that this code snippet is independent of both  $\pi$  and  $k$ , so that these somewhat tedious calculations need be performed only once per manifold.

**Choice of Kernel** To proceed we require a reproducing kernel  $k$  defined on  $S^2$ . To this end, recall the generalised hypergeometric function

$$z \mapsto {}_pF_q \left[ \begin{matrix} a_1, \dots, a_p \\ b_1, \dots, b_q \end{matrix} ; z \right]$$

and the fact that this satisfies

$$\frac{d}{dz} {}_pF_q \left[ \begin{matrix} a_1, \dots, a_p \\ b_1, \dots, b_q \end{matrix} ; z \right] = \frac{\prod_{i=1}^p a_i}{\prod_{j=1}^q b_j} {}_pF_q \left[ \begin{matrix} a_1 + 1, \dots, a_p + 1 \\ b_1 + 1, \dots, b_q + 1 \end{matrix} ; z \right].$$

Recall also the Pochhammer symbol  $(z)_n := \Gamma(z+n)/\Gamma(z)$ . Proposition 5 of Brauchart and Dick (2013) establishes that, for  $\alpha \in \mathbb{N} + \frac{1}{2}$ , the kernel

$$k(\mathbf{x}, \mathbf{y}) = C_{1,m,\alpha} {}_3F_2 \left[ \begin{matrix} \frac{3}{2} - \alpha, 1 - \alpha, \frac{3}{2} - \alpha \\ 2 - \alpha, 3 - \frac{m}{2} - 2\alpha \end{matrix} ; \frac{1 - \mathbf{x} \cdot \mathbf{y}}{2} \right] + C_{2,m,\alpha} \|\mathbf{x} - \mathbf{y}\|^{2\alpha-2},$$

defined for  $\mathbf{x}, \mathbf{y} \in S^m$ , reproduces the Sobolev space  $H^\alpha(S^m)$ . The constant terms here are

$$\begin{aligned} C_{1,m,\alpha} &= \frac{2^{2\alpha-2} (\frac{m}{2})_{2\alpha-2}}{2\alpha - 2 (m)_{2\alpha-2}} \\ C_{2,m,\alpha} &= (-1)^{\alpha-\frac{1}{2}} 2^{1-2\alpha} \frac{\Gamma(\frac{m+1}{2})\Gamma(\alpha - \frac{1}{2})\Gamma(\alpha - \frac{1}{2})}{\sqrt{\pi}\Gamma(\frac{m}{2})(\frac{1}{2})_{\alpha-\frac{1}{2}}(\frac{m}{2})_{\alpha-\frac{1}{2}}}. \end{aligned}$$

This kernel was used in our experiments, with values  $\alpha \in \{7/2, 9/2, 11/2\}$  considered.

**Experimental Results** To illustrate the method, consider the von Mises-Fisher distribution  $\mathcal{P}$  whose density with respect to  $\mathcal{H}$  is

$$\pi_{\mathcal{P}}(\mathbf{x}) = \frac{\|\mathbf{c}\|_2}{4\pi \sinh(\|\mathbf{c}\|_2)} \exp\{\mathbf{c}^\top \mathbf{x}\}.$$

The fact that this is a density on  $S^2$  can be directly verified by checking that

$$\int_{q_1=0}^{2\pi} \int_{q_2=0}^{\pi} \pi_{\mathcal{P}}(\nu(\mathbf{q})) \sin q_2 \, dq_1 dq_2 = 1.$$

For illustration we suppose that the normalisation constant is unknown and we have access only to  $\pi(\mathbf{x}) = \exp\{\mathbf{c}^\top \mathbf{x}\}$ . Thus we proceed to construct the differential operator operator  $L_\pi$  as previously described.

To gain intuition as to the reasonableness of the resulting  $k_\pi$ , we fixed  $\alpha = 7/2$  and plotted the first few eigenfunctions of  $k_\pi$  for the target distribution  $\pi_{\mathcal{P}}$  defined by  $\mathbf{c} = [1, 0, 0]$ . These are shown in Fig. 5. Note that, in simple visual terms, these seem like a reasonable basis in which to perform function approximation on  $S^2$ .

Next, we considered the performance of the proposed integration method. For various values of  $n$ , we obtained  $n$  points  $\{\mathbf{x}_i\}_{i=1}^n$  that were quasi-uniformly distributed on  $S^2$ , being obtained<sup>1</sup> by minimising a generalised electrostatic potential energy (i.e., Reisz’s-energy). Note that these points, being uniform, do not form an approximation to  $\mathcal{P}$ . For each point set we computed the worst case error in Eqn. 4.

---

<sup>1</sup>code due to Anton Semechko; “Suite of functions to perform uniform sampling of a sphere” on the MATLAB file exchange server.



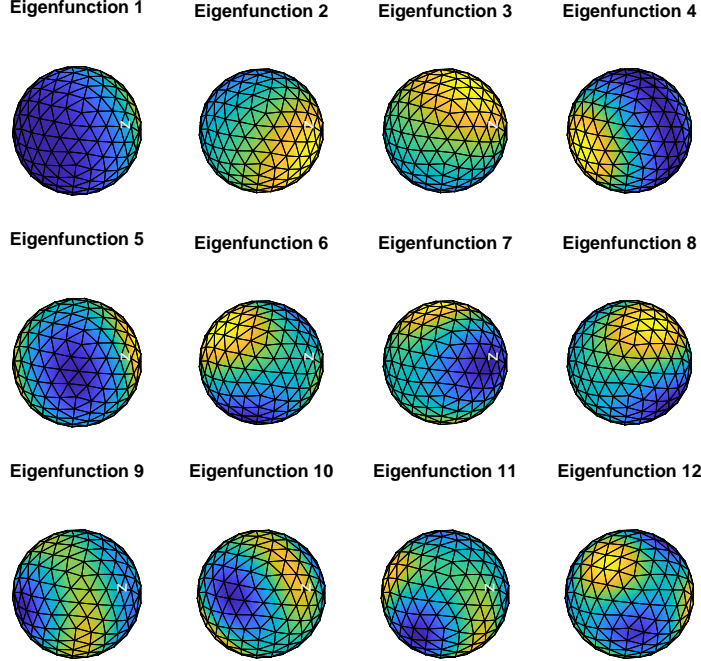


Figure 5: The first twelve eigenfunctions of the kernel  $k_\pi$  for a von Mises-Fisher distribution on  $S^2$ .

Results in Fig. 6 showed that the worst case error decays more rapidly with larger  $\alpha$ . Again, we see a clear improvement compared to the  $O_P(n^{-1/2})$  of MCMC. Although it is not possible to accurately read off asymptotic rates from these results, they are somewhat consistent with a convergence rate of  $O(n^{-(\alpha-2)/d})$  where  $d = 2$ . This conjecture is more speculative than the rates conjectured for the Euclidean manifold.

## 5 Discussion

This note presented a generalisation of the method of Oates et al. (2016, 2017) for posterior integration on an embedded Riemannian manifold. The presentation was informal and leaves scope for a subsequent more technical treatment. In particular, three central open theoretical questions are (1) how expressive is the function class  $H_\pi$  in general (2) how quickly do these estimators converge under particular regularity assumptions on the integrand, and (3) how robust are these estimators when the function space assumptions are violated?

The experimental results that we presented were designed to be both transparent and reproducible, but as a consequence the experiments themselves were not as challenging as the numerical integration tasks that one would typically encounter in the applied context. Further empirical work will be needed to assess the proposed methods on a variety of posterior integrals. In particular, the case of high-dimensional manifolds (i.e.  $m$  large) is likely to

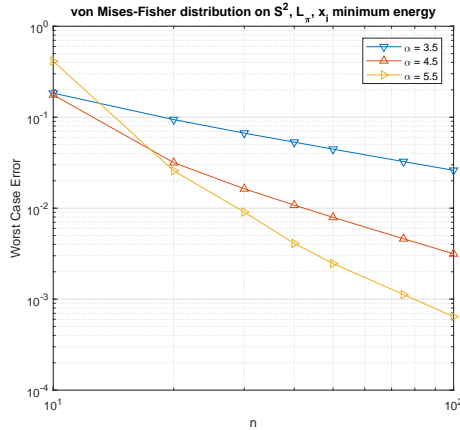


Figure 6: Results for the von Mises-Fisher distribution on  $S^2$ . The worst case error of the proposed method is plotted for various  $\alpha$ , controlling the smoothness of the kernel, and various  $n$ , the number of evaluations of the integrand. [The points  $\mathbf{x}_i$  were quasi-uniform over  $S^2$  and the differential operator  $L_\pi$  was used.]

challenge any regression-based method unless very strong assumptions can be made on the integrand.

A practical weakness of the proposed method is that it relies on the availability of a kernel, or family of kernels, that are defined on the given manifold. However, the stochastic partial differential approach (Fasshauer and Ye, 2011; Lindgren et al., 2011) could perhaps be used to numerically approximate a suitable kernel. Related, the kernel can be chosen in such a way that the  $O(n^3)$  cost of solving the linear system  $\mathbf{K}_\pi^{-1}\mathbf{1}$  is reduced, for instance by using a compact support.

**Related Work** In the same week that this note was finished, similar results appeared on arXiv in Liu and Zhu (2017). That work considered the same differential operator  $L_\pi$ , but after that point the two papers diverge, with Liu and Zhu (2017) pursuing a Riemannian manifold generalisation of Stein variation gradient descent (Liu and Wang, 2016) called RSVGd. Nevertheless, Liu and Zhu (2017) provide a thorough treatment of the differential geometry and it would be interesting to compare our proposed method with RSVGd in future work.

## References

- Assaraf, R. and Caffarel, M. (1999). Zero-variance principle for Monte Carlo algorithms. *Physical Review Letters*, 83(23):4682.
- Atkinson, K. (1982). Numerical integration on the sphere. *The ANZIAM Journal*, 23(3):332–347.

- Bachman, D. (2006). *A Geometric Approach to Differential Forms*. Birkhäuser.
- Berlinet, A. and Thomas-Agnan, C. (2011). *Reproducing kernel Hilbert spaces in probability and statistics*. Springer Science & Business Media.
- Bernardo, J. M. and Smith, A. F. M. (2001). *Bayesian Theory*. IOP Publishing.
- Brandolini, L., Choirat, C., Colzani, L., Gigante, G., Seri, R., and Travaglini, G. (2010). Quadrature rules and distribution of points on manifolds. *arXiv:1012.5409*.
- Brauchart, J. S. and Dick, J. (2013). A characterization of Sobolev spaces on the sphere and an extension of Stolarsky’s invariance principle to arbitrary smoothness. *Constructive Approximation*, 38(3):397–445.
- Briol, F.-X., Oates, C. J., Girolami, M., Osborne, M. A., and Sejdinovic, D. (2016). Probabilistic integration: A role in statistical computation? *arXiv:1512.00933*.
- Byrne, S. and Girolami, M. (2013). Geodesic Monte Carlo on embedded manifolds. *Scandinavian Journal of Statistics*, 40(4):825–845.
- Chwialkowski, K., Strathmann, H., and Gretton, A. (2016). A kernel test of goodness of fit. In *ICML*.
- Diaconis, P., Holmes, S., and Shahshahani, M. (2013). Sampling from a manifold. In *Advances in Modern Statistical Theory and Applications: A Festschrift in honor of Morris L. Eaton*, pages 102–125. Institute of Mathematical Statistics.
- Ehler, M. and Gräf, M. (2017). Optimal Monte Carlo integration on closed manifolds. *arXiv:1707.04723*.
- Fasshauer, G. (2007). *Meshfree Approximation Methods with MATLAB*. World Scientific.
- Fasshauer, G. E. and Ye, Q. (2011). Reproducing kernels of generalized Sobolev spaces via a Green function approach with distributional operators. *Numerische Mathematik*, 119(3):585–611.
- Federer, H. (1969). *Geometric Measure Theory*. Springer.
- Filbir, F. and Mhaskar, H. N. (2010). A quadrature formula for diffusion polynomials corresponding to a generalized heat kernel. *Journal of Fourier Analysis and Applications*, 16(5):629–657.
- Friel, N. and Wyse, J. (2012). Estimating the evidence—a review. *Statistica Neerlandica*, 66(3):288–308.
- Gorham, J., Duncan, A. B., Vollmer, S. J., and Mackey, L. (2016). Measuring sample quality with diffusions. *arXiv:1611.06972*.

- Gorham, J. and Mackey, L. (2017). Measuring sample quality with kernels. In *ICML*.
- Gräf, M. (2013). *Efficient algorithms for the computation of optimal quadrature points on Riemannian manifolds*. PhD thesis, Universitätsverlag der Technischen Universität Chemnitz.
- Holbrook, A., Lan, S., Vandenberg-Rodes, A., and Shahbaba, B. (2016). Geodesic Lagrangian Monte Carlo over the space of positive definite matrices: with application to Bayesian spectral density estimation. *arXiv:1612.08224*.
- Kuo, F. Y. and Sloan, I. H. (2005). Quasi-Monte Carlo methods can be efficient for integration over products of spheres. *Journal of Complexity*, 21(2):196–210.
- Lan, S., Zhou, B., and Shahbaba, B. (2014). Spherical Hamiltonian Monte Carlo for constrained target distributions. In *ICML*, pages 629–637.
- Lindgren, F., Rue, H., and Lindström, J. (2011). An explicit link between Gaussian fields and Gaussian Markov random fields: The stochastic partial differential equation approach. *Journal of the Royal Statistical Society: Series B*, 73(4):423–498.
- Liu, A. and Lee, J. D. (2017). Black-box importance sampling. In *AISTATS*.
- Liu, C. and Zhu, J. (2017). Riemannian Stein Variational Gradient Descent for Bayesian Inference. *arXiv:1711.11216*.
- Liu, Q., Lee, J., and Jordan, M. (2016). A Kernelized Stein Discrepancy for Goodness-of-fit Tests and Model Evaluation. In *ICML*.
- Liu, Q. and Wang, D. (2016). Stein variational gradient descent: A general purpose Bayesian inference algorithm. In *NIPS*, pages 2378–2386.
- Mardia, K. V. and Jupp, P. E. (2000). *Directional Statistics*. John Wiley & Sons.
- Marzouk, Y., Moselhy, T., Parno, M., and Spantini, A. (2016). An introduction to sampling via measure transport. *arXiv:1602.05023*.
- Meyn, S. P. and Tweedie, R. L. (2012). *Markov chains and stochastic stability*. Springer Science & Business Media.
- Mira, A., Solgi, R., and Imparato, D. (2013). Zero variance Markov chain Monte Carlo for Bayesian estimators. *Statistics and Computing*, 23(5):653–662.
- Oates, C. J., Cockayne, J., Briol, F.-X., and Girolami, M. (2016). Convergence rates for a class of estimators based on Stein’s identity. *arXiv:1603.03220*.
- Oates, C. J., Girolami, M., and Chopin, N. (2017). Control functionals for monte carlo integration. *Journal of the Royal Statistical Society: Series B (Statistical Methodology)*, 79(3):695–718.

- Philippe, A. and Robert, C. P. (2001). Riemann sums for MCMC estimation and convergence monitoring. *Statistics and Computing*, 11(2):103–115.
- Porcu, E., Bevilacqua, M., and Genton, M. G. (2016). Spatio-temporal covariance and cross-covariance functions of the great circle distance on a sphere. *Journal of the American Statistical Association*, 111(514):888–898.
- Rasmussen, C. E. and Williams, C. K. (2006). *Gaussian Processes for Machine Learning*. MIT Press.
- Schölkopf, B., Herbrich, R., and Smola, A. (2001). A generalized representer theorem. In *COLT*.
- Schwab, C. and Stuart, A. M. (2012). Sparse deterministic approximation of Bayesian inverse problems. *Inverse Problems*, 28(4):045003.
- Spivak, M. (1971). *Calculus on manifolds: A modern approach to classical theorems of advanced calculus*. Westview Press.
- Stuart, A. M. (2010). Inverse problems: A Bayesian perspective. *Acta Numerica*, 19:451–559.